Journal of Thermal Analysis and Calorimetry, Vol. 96 (2009) 1, 267–276

THERMAL STUDIES OF Co(II), Ni(II) AND Cu(II) COMPLEXES OF N,N'-*bis*(3,5-Di-*t*-BUTYLSALICYLIDENE)ETHYLENEDIAMINE

F. Doğan[1*], *M. Ulusoy*[2], *Ö. F. Öztürk*[1,3], *İ. Kaya*[1] *and B. Salih*[3]

[1]Çanakkale Onsekiz Mart University, Faculty of Arts and Science, Chemistry Department, Çanakkale, Turkey
[2]Ege University, Faculty of Science, Chemistry Department, İzmir, Turkey
[3]Hacettepe University, Faculty of Science, Chemistry Department, Ankara, Turkey

The thermal decomposition kinetics of sterically hindered salen type ligand (**L**) and its metal complexes [*M*=Co(II), Ni(II), Cu(II)] were investigated by thermogravimetric analysis. A direct insertion probe-mass spectrometer (DIP-MS) was used for the characterization of metal complexes of **L** and all fragmentations and stable ions were characterized. The thermogravimetry and differential thermogravimetry (TG-DTG) plots of salen type salicylaldimine ligand and complexes showed a single step.

The kinetic analysis of thermogravimetric data was performed by using the invariant kinetic parameter method (IKP). The values of the invariant activation energy, E_{inv} and the invariant pre-exponential factor, A_{inv}, were calculated by using Coats–Redfern (CR) method. The thermal stabilities and activation energies of metal complexes of sterically hindered salen type ligand (**L**) were found as Co(II)>Cu(II)>Ni(II)>**L** and $E_{Cu}>E_{Ni}>E_{Co}>$**L**. Also, the probabilities of decomposition functions were investigated. The diffusion functions (D_n) are most probable for the thermal decomposition of all complexes.

Keywords: *activation energy, sterically hindered Schiff base, thermal decomposition kinetic, thermogravimetry*

Introduction

The coordination chemistry of salen type salicylaldimine ligands with metal complexes have some interesting applications, e.g. in catalytic oxidation reactions and electrochemical reduction processes [1], in metalloenzyme-mediated catalysis [2], metal-containing liquid-crystalline polymers [3] and as catalytically active materials to develop surface-modified electrodes [4]. It is known that sterically hindered ligands bearing salicylaldimines are effective antioxidant and widely used in rancidification of fats and oils [5]. In recent years, manuscripts dealing with thermal analysis of salen type salicylaldimine ligands with metal complexes are insufficient. The determination of kinetic parameter from data of non-isothermal thermogravimetry is one of the most difficult kinetic problems. Considerable attention is paid to the kinetic parameters calculation from TG curves. Many authors investigated the kinetic data analysis of complexes by integral, differential and specified methods. Also, new calculation methods are still being published [6, 7]. A number of papers are devoted to comparing these methods [8–11] or to their critical assessment [12]. Soliman [13] has investigated the thermal stabilities of the chromium and molybdenum complexes with salicylidene-2-aminophenol, salicylidene-2-aminoanisole, salicylidene-2-aminoaniline and biquinoline. Thermal decomposition of some linear trinuclear Schiff base complexes with acetate bridges have been studied by Durmuş *et al*. [14]. Yeşilel [15], Mohamed *et al*. [16] and Doğan *et al*. [17] have investigated the thermal behavior, kinetic and thermodynamic parameters of the metal complexes and salts with imidazole and benzimidazole in various atmosphere using TG/DTG, DTA and elemental analytical methods. In this paper, salen type ligand and its Cu(II) [18], Ni(II) [19] and Co(II) complexes were synthesized according to the published literature and investigated their thermal properties. We use a method developed by Lesnikovich *et al*. [20] at different heating rates to compute invariant kinetic parameters (IKP) of salen type ligand and its metal complexes, which have usually been applied to study the decomposition of polymeric materials from thermogravimetric data.

Experimental

Preparation of samples

Metal solutions of Co(II), Ni(II) and Cu(II) ions are prepared from analytical purity reagents of $Co(CH_3COO)_2{\cdot}4H_2O$, $Ni(CH_3COO)_2{\cdot}4H_2O$ and $Cu(CH_3COO)_2{\cdot}H_2O$ salts. Metal complexes (CoL, CuL and NiL) are obtained from the reactions of metal solutions with alcoholic (ethanol) ligand solutions. The

* Author for correspondence: fatihdogan@comu.edu.tr

1388–6150/$20.00

Akadémiai Kiadó, Budapest, Hungary
Springer, Dordrecht, The Netherlands

analytical data and also FTIR results of CuL and NiL complexes are compatible with reported literature [18, 19]. Solid metal complexes were filtered in vacuum and recrystallized from dichloromethane/ethanol (*v*/*v*; 1/3). For Cu(II) complex: Yield: 85%; *M.p.*>270°C; ν_{max} (KBr Disk) (cm^{-1}) 3033 (Ar-CH); 2985–2863 (Al-CH); 1615 (C=N); μ_{eff}: 1.92 [B.M.]; λ_{max} (nm) (logε, M^{-1} L^{-1}) in $CHCl_3$: 300, 323 (4.19), 397 (4.11), 480a, 634 (2.42); Anal. found: C, 69.12; H, 7.88; N, 4.46. Calc. for $C_{32}H_{46}N_2O_2Cu$: C, 69.34; H, 8.37; N, 5.05%. For Ni(II) complex: Yield: 87%; *M.p.*>270°C; ν_{max} (KBr Disk) (cm^{-1}) 3028 (Ar-CH); 2992–2881 (Al-CH); 1620 (C=N); μ_{eff}: diamagnetic; λ_{max} (nm) (logε, M^{-1} L^{-1}) in $CHCl_3$: 270 (4.37), 330 (3.98), 407 (3.80), 648 (2.19); Anal. found: C, 70.35; H, 8.39; N, 5.33. Calc. for $C_{32}H_{46}N_2O_2CuNi$: C, 69.96; H, 8.44; N, 5.10%.

Synthesis of Co(II) complex of N,N'-*bis*(3,5-di-*t*-butylsalicylidene)-1,3-ethylenediamine

The 1 mmol Schiff base ligand dissolved in hot ethanol (25 mL) and the appropriate 1 mmol $Co(OAc)_2 \cdot 4H_2O$ was added under an argon atmosphere over a few minutes causing the precipitation of the orange product. The reaction was allowed to cool to room temperature and stirred (3 h). The product was isolated by filtration from the reaction mixture and dried under vacuum. Recrystallized from dichloromethane/ethanol (*v*/*v*; 1/3). Yield: 72%; *M.p*. 201–205°C; ν_{max} (KBr Disk) (cm^{-1}) 3043 (Ar-CH); 2953–2868 (Al-CH); 1620 (C=N); μ_{eff}: 4.05 [B.M.], *S*=3/2 in Td.; Anal. found: C, 70.67; H, 8.95; N, 5.23. Calc. for $C_{32}H_{46}N_2O_2Co$: C, 69.92; H, 8.44; N, 5.10%.

Instrumentation

All thermal analysis work were performed on Perkin Elmer Termogravimetric Analyzer Pyris-6, operating in dynamic mode, with the following conditions; sample mass ~5 mg, heating rate=5, 10, 15, 20°C min^{-1}, atmosphere of nitrogen (10 cm^3 min^{-1}), sealed platinum pan. All kinetic experiments were carried in duplicate and reproducible results with the smaller variations in the kinetic parameters were obtained. **L** and its metal ion complexes, such as Cu(II), Ni(II) and Co(II)-complexes, were analyzed using an Agilent 5973 Inert Mass Selective Detector equipped with Direct Insertion Probe (HPP7&ProbeDirect, Scientific Instrument Services, Ringoes, NJ USA). About 1 mg of the ligand and its complexes were weighted and then inserted inside the quartz sample tube (Scientific Instrument Services, Ringoes, NJ USA) that was used for inserting the sample inside mass spectrometer. At the mass spectrometer, Electron Impact Ionization (EI) source was used, the temperature of the source was set to 140°C, vacuum was $1.5 \cdot 10^{-6}$ Torr during the recording of mass spectra. The Direct Insertion Probe program was set as given below:

Initial temperature was set to 50°C for 10 min and then temperature was increased up to 420°C with 10°C min^{-1} temperature ramp. Finally temperature held at 420°C for 50 min.

Results and discussion

Thermal behaviour and GC-MS analysis of Schiff base and its metal complexes

The thermal behavior of **L** and its metal-complexes [Co(II), Cu(II) and Ni(II)] at different heating rates 5, 10, 15, 20°C min^{-1} are presented in Figs 1–4, respectively. As seen in Figs 1–4, each TG curves for both **L** and its metal-complexes exhibits one stage decomposition. The TG curve of all the compounds show a similar characterizations. The thermal decomposition products, the temperature range concerned (initial, T_i and final, T_f), the percentage of mass lost during the decomposition, the maximum decomposition temperature (T_m) and the theoretical percentage of mass lost calculated from TG curve at heating rate of 5°C min^{-1} are listed in Table 1 for both **L** and its metal complexes.

Table 1 T_i, T_m and T_f values of **L**, CoL, CuL and NiL for the heating rate of 5°C min^{-1}

Complex	Step	DTG_{max}/°C	Temperature range/°C	Mass loss/%,		Assignment
				found	(calc.)	
L	I	278	204–293	100	100	$C_{32}H_{48}N_2O_2$
	residue	>293				
CoL	I	401	319–420	85.2	86.4	$C_{32}H_{46}N_2O_2Co$
	residue	>420		13.1	13.6	CoO
CuL	I	395	297–412	84.1	85.7	$C_{32}H_{46}N_2O_2Cu$
	resideu	>412		13.5	14.3	CuO
NiL	I	376	290–395	85.9	86.4	$C_{32}H_{46}N_2O_2Ni$
	residue	>395		12.2	13.6	NiO

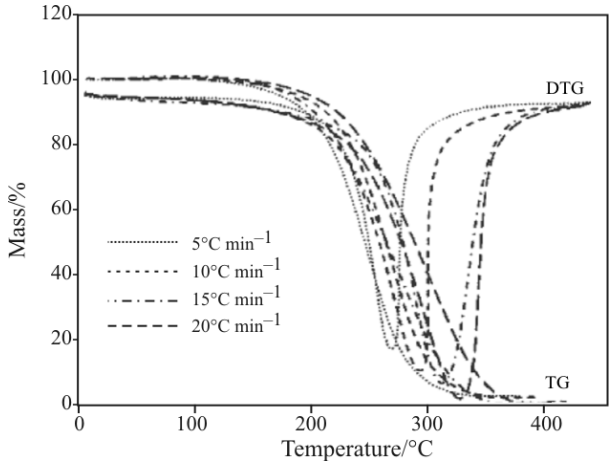

Fig. 1 TG/DTG curves of **L** at different rates

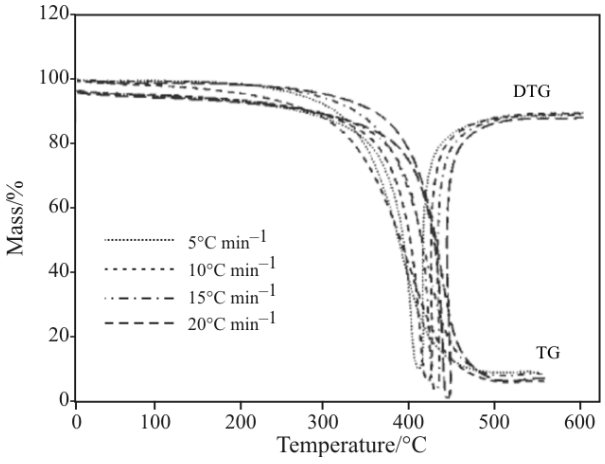

Fig. 2 TG/DTG curves of CuL at different rates

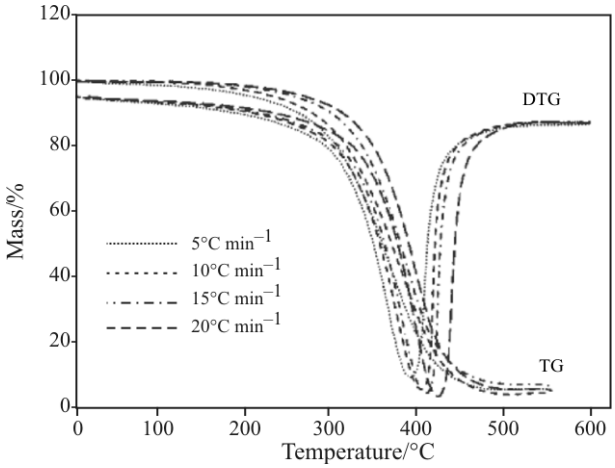

Fig. 3 TG/DTG curves of CoL at different rates

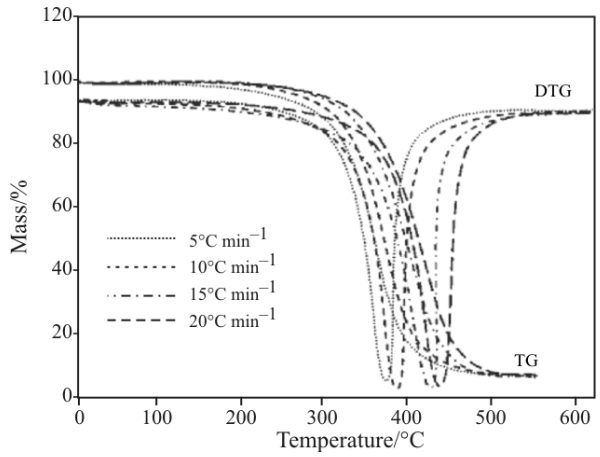

Fig. 4 TG/DTG curves of NiL at different rates

There is mainly one stage of decomposition of **L** and its metal complexes for all the heating rates investigated and a higher heating rate shifts the rate curve to a higher temperature.

Also, in order to check the thermal stability of the complexes in the solid state, initial temperatures of the decomposition of **L** and its complexes were compared. It was found that the thermal stabilities of ligand and its metal complexes follow the order Co(II)>Cu(II)>Ni(II)>**L**. In literature, it was found by Arshad *et al*. that thermal stabilities of 1,2-dipiperidinoethane complexes of cobalt, nickel, zinc and cadmium, increase in the following sequence: Ni(II)< Co(II)<Cu(II)<Zn(II)<Cd(II) [21]. On the other hand, in another study, the thermal stabilities of metal complexes of the 6-(2-pyridylazo-acetamidophenol were found as Ni(II)>Cu(II)>Zn(II)>Fe(II)>Co(II) [22]. Consequently, it is believed that the coordination of the metal ions to ligands is responsible for thermal stabilities of the metal complexes. The solid residue of thermal decomposition of all the complexes was metal oxide. The characterization of the end products

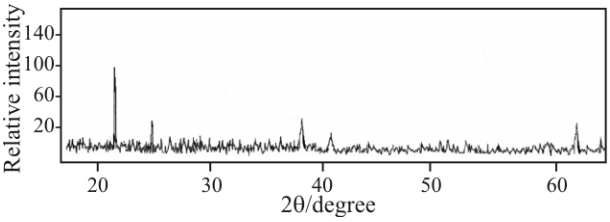

Fig. 5 X-ray powder diffraction pattern of CoO

of the decomposition was achieved by X-ray diffraction. An as example the X-ray pattern of the end product of Co(II) complexes is shown in Fig. 5. These results conformed to our previous work [23].

Mass spectrum of ligand (**L**) is given in Fig. 6 with the total ion chromatogram of **L**. On the total ion chromatogram, beside the main peak of the ligand obtained at 3.9 min retention time, some other degradation peaks were observed. When the mass spectrum of the main peak on total ion chromatogram was evaluated, it was noticed that this compound pointed out the mass spectrum of L exactly. In the mass spectrum given in Fig. 6B, the peaks appeared at 492, 477, 260,

Table 2 Mass and intensity (%) of the peaks were evaluated from mass spectra of the studied complexes

Co(II) complex			Ni(II) complex			Cu(II) complex		
Nominal	Intensity	Type of ion	Nominal mass	Intensity	Type of ion	Nominal	Intensity	Type of ion
549	100	M^+	548	100	M^+	553	100	M^+
534	57	$[M-15]^+$	533	86.4	$[M-15]^+$	261	78.8	$[M-15-15]^{2+}$
260	57.6	$[M-15-15]^{2+}$	259	82.6	$[M-15-15]^{2+}$	538	41.8	$[M-15]^+$
246	9.4	$[C_{16}H_{24}NO]^+$	550	44.1	$[M+2]^+$	244	16.2	$[C_{16}H_{24}NO]^+$
518	5.0	$[M-15-16]^+$	535	38.5	$[M-15+2]^+$	229	9.1	$[C_{17}H_{24}NO-15-25]^+$
258	6.2	$[C_{17}H_{24}NO]$	260	33.7	$[M-15]^+$?	216	8.0	$[C_{14}H_{18}NO]^+$
231	3.1	$[L-15-15]^+$	57	25.9	$[(CH_3)_3C]^+$	57	8.5	$[(CH_3)_3C]^+$
267	7.2		231	11.4	$[L-15-15]^+$	272	8.8	

259, 244, 231, 218 and 57 atomic masses characterized the M^+, $[M-15]^+$, $[C_{17}H_{26}NO]^+$, $[C_{17}H_{25}NO]^+$, $[C_{17}H_{25}NO-15]^+$, $[M-15-15]^{2+}$, $[C_{17}H_{25}NO-15-26]^+$ and $[(CH_3)_3C]^+$. Especially, the peak at 231 atomic mass with high intensity is really interesting and representing very stable doubly charged ion of the ligand in EI-mass spectrometry which is unexpected. Doubly charged ion stability is because of the high volume of ligand in the space and the charged locations are enough far away from each other to eliminate the same charged center repulsions.

When mass spectra of metal complexes of this ligand were interpreted, similar fragmentations were observed but doubly charged ion intensity of the complexes accompanied two methyl groups elimination from both bulky sides of the complexes were found to be higher than the intensity of the same peak of pure ligand. For the metal complexes, the mass of the peaks observed on mass spectra with their per cent intensities are given in Table 2. In order to evaluate the high intense doubly charged ion further, mass spectra of nickel complex of **L** with the total ion mass chromatogram of the complex is given in Fig. 7. Chosen the nickel complex is the reason of the intense isotopic mass distribution of nickel in the complex. Evaluating the isotopic peak masses and intensities of nickel in either single charge molecular ion or doubly charged ion form, existing of doubly charged ion in the spectrum could be examined clearly. Single charged molecular ion at 548 and at 550 nominal masses are the M^+ and $[M+2]^+$ characterizing the highest abundant nickel isotopes which have 58 Ni and 60 Ni with 68.08 and 26.22% naturally abundance. The doubly charged ion of the complex formed with leaving of two methyl groups from both bulky sides of the complex yielded again two peaks appeared at 260 and 259 nominal masses showing again nickel isotope distribution

Except ^{13}C isotope addition. These results clearly show that complex yields high intense (very stable) doubly charged ion loosing two methyl groups.

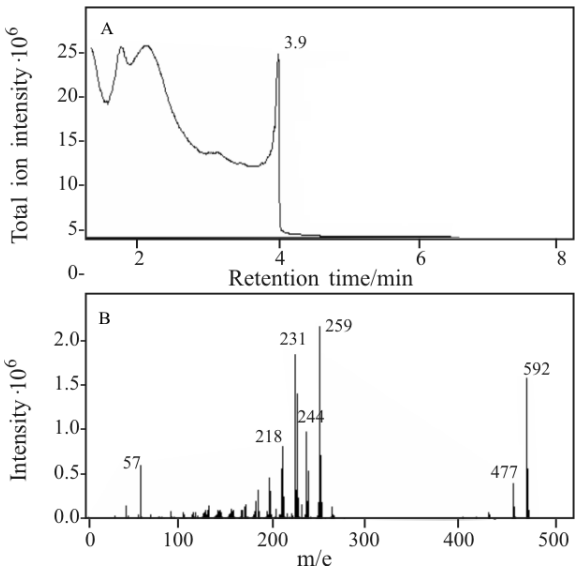

Fig. 6 A – Total ion chromatogram and B – mass spectrum of ligand. Mass spectrum was obtained at 3.9 retention time

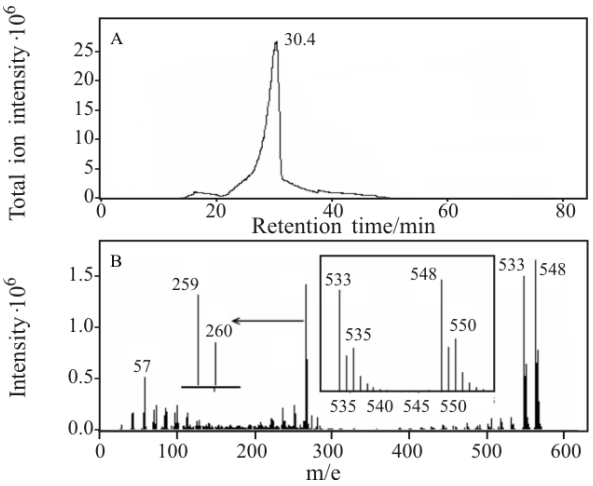

Fig. 7 A – Total ion chromatogram and B – mass spectrum of L-Ni(II) complex. Mass spectrum was obtained at 30.4 retention time

Kinetic parameters

IKP method

Any kinetic analysis of solid state decomposition is usually based on the rate equation

$$\frac{d\alpha}{dt} = kf(\alpha) \quad (1)$$

where α is the degree of conversion, t retention time and $f(\alpha)$ the differential function of conversion. This function may take various forms, some of which are shown in Table 3 [24, 25].

The explicit temperature dependence of the rate constant is introduced by replacing $k=A\exp(-E_a/RT)$ with the Arrhenius law, which gives

$$\frac{d\alpha}{dt} = A\exp\left(\frac{-E_a}{RT}\right)f(\alpha) \quad (2)$$

where A is the pre-exponential factor (s^{-1}), E_a the activation energy (J mol^{-1}) and R the gas constant (J mol^{-1} K^{-1}). When the reaction is carried out by controlling the temperature ($T=T_0+\beta t$, where β is the linear heating rate and T_0 the starting temperature) Eq. (2) may be written as

$$\frac{d\alpha}{dT} = \frac{A}{\beta}\exp\left(\frac{-E_a}{RT}\right)f(\alpha) \quad (3)$$

The thermal decomposition of a solid in a heterogeneous process is accompanied by the release of gaseous products can usually be characterized by several forms of the function $f(\alpha)$ given in Table 3. The invariant kinetic parameter method is based on the relation of the compensation effect which described by the values of activation parameters E_a, and pre-exponential factors A, obtained from various conversion function using one of different methods (differential or integral methods, etc.) for TG curves. To apply this method, $\alpha=\alpha(T)$ curves for several heating rates (β_v, v=1,2,3) are recorded and the activation parameters E_a and pre-exponential factors A for a set of conversion function ($f_j(\alpha)$, j=1,2,3..), at each heating rates are calculated using an integral, differential method and other method. In this work, the CR method [26] was used to integrate Eq. (3). It leads to the following relations:

$$\ln\frac{g_j(\alpha_{iv})}{T_{iv}^2} \cong \ln\frac{A_{jv}R}{\beta_v E_{a\,jv}} - \frac{E_{a\,jv}}{RT_{iv}} \quad (4)$$

with

Table 3 $f(\alpha)$ and $g(\alpha)$ functions used in the invariant kinetic parameter method

No.	Mechanisms	Symbol	Differential form, $f_j(\alpha)$	Integral form, $g_j(\alpha)$
1	N and G (n=1)	S1	$4(1-\alpha)[-\ln(1-\alpha)]^{3/4}$	$[-\ln(1-\alpha)]^{1/4}$
2	N and G (n=1.5)	S2	$3(1-\alpha)[-\ln(1-\alpha)]^{2/3}$	$[-\ln(1-\alpha)]^{1/3}$
3	N and G (n=2)	S3	$2(1-\alpha)[-\ln(1-\alpha)]^{1/2}$	$[-\ln(1-\alpha)]^{1/2}$
4	N and G (n=3)	S4	$(3/2)(1-\alpha)[-\ln(1-\alpha)]^{1/3}$	$[-\ln(1-\alpha)]^{2/3}$
5	N and G (n=4)	S5	$(1-\alpha)$	$[-\ln(1-\alpha)]$
6	Contracted geometry shape (contracting linear)	S6	1	α
7	Contracted geometry shape (cylindrical symmetry)	S7	$2(1-\alpha)^{1/2}$	$2[1-(1-\alpha)^{1/2}]$
8	Contracted geometry shape (sphere symmetry)	S8	$3(1-\alpha)^{2/3}$	$3[1-(1-\alpha)^{1/3}]$
9	Diffusion, 1D	S9	$1/(2\alpha)$	α^2
10	Diffusion, 2D	S10	$1/(\ln(1-\alpha))$	$(1-\alpha)\ln(1-\alpha)+\alpha$
11	Diffusion, 3D	S11	$1.5/[(1-\alpha)^{-1/3}-1]$	$(1-2\alpha/3)-(1-\alpha)^{2/3}$
12	Diffusion, 3D	S12	$[1.5(1-\alpha)^{2/3}][1-(1-\alpha)^{1/3}]^{-1}$	$[1-(1-\alpha)^{1/3}]^2$
13	Diffusion, 3D	S13	$(3/2)(1+\alpha)^{2/3}[(1+\alpha)^{1/3}-1]^{-1}$	$[(1+\alpha)^{1/3}-1]^2$
14	Diffusion, 3D	S14	$(3/2)(1-\alpha)^{4/3}[1/(1-\alpha)^{1/3}-1]^{-1}$	$[[1/(1-\alpha)]^{1/3}-1]^2$
15	Mample power law	S15	$4\alpha^{3/4}$	$\alpha^{1/4}$
16	Mample power law (n=3)	S16	$(1.5)\alpha^{2/3}$	$\alpha^{1/3}$
17	Mample power law (n=2)	S17	$2\alpha^{1/2}$	$\alpha^{1/2}$
18	Mample power law (n=3/2)	S18	$3/2(\alpha)^{1/3}$	$\alpha^{2/3}$
19	Mample power law (n=2/3)	S19	$2/3(\alpha)^{-1/2}$	$\alpha^{3/2}$
20	Mample power law (n=4/3)	S20	$4/3(\alpha)^{-1/3}$	$\alpha^{3/4}$
21	Chemical reaction (n=2)	S21	$(1-\alpha)^2$	$(1-\alpha)^{-1}-1$
22	Chemical reaction (n=1/2)	S22	$2(1-\alpha)^{1/2}$	$1-(1-\alpha)^{1/2}$
23	Chemical reaction (n=1/3)	S23	$3(1-\alpha)^{2/3}$	$1-(1-\alpha)^{1/3}$

Table 4 Apparent conversion parameters of **L** obtained for various conversation functions by means of IKP method

Heating rate	5°C min^{-1}		10°C min^{-1}		15°C min^{-1}		20°C min^{-1}	
Function	E_a/kJ mol^{-1}	ln$A$/s^{-1}	E_a/kJ mol^{-1}	ln$A$/s^{-1}	E_a/kJ mol^{-1}	ln$A$/s^{-1}	E_a/kJ mol^{-1}	ln$A$/s^{-1}
S1	18.890	0.860	21.250	1.970	16.910	1.090	15.460	0.930
S2	28.110	3.280	31.380	4.500	25.640	3.320	23.720	3.050
S3	46.540	7.820	51.630	9.290	43.110	7.460	40.230	6.950
S4	64.970	12.19	71.890	13.92	60.570	11.41	56.750	10.68
S5	101.83	20.72	112.39	22.95	95.500	19.10	89.790	17.89
S6	76.510	14.37	80.210	15.23	69.120	12.77	64.910	11.95
S7	88.000	17.27	94.260	18.62	80.880	15.61	75.910	14.59
S8	92.340	18.35	99.810	19.95	85.410	16.70	80.190	15.61
S9	161.77	33.29	169.54	34.35	147.54	29.23	139.14	27.33
S10	175.80	36.05	186.24	37.60	161.69	31.87	152.33	29.73
S11	181.60	35.97	193.55	37.82	167.72	31.77	158.00	29.55
S12	193.43	38.86	208.75	41.37	180.11	34.66	169.70	32.27
S13	148.52	27.76	155.03	28.65	134.81	23.97	127.36	22.30
S14	233.64	48.65	263.14	54.02	223.25	44.65	210.87	41.78
S15	12.565	–1.06	13.210	–0.34	10.310	–0.89	9.2400	–0.99
S16	19.670	0.900	20.650	1.620	16.850	0.900	15.430	0.740
S17	33.881	4.470	35.540	5.230	29.920	4.090	27.800	3.760
S18	48.090	7.850	50.430	8.640	42.980	7.070	40.170	6.570
S19	119.13	23.90	124.87	24.86	108.33	21.07	102.02	19.70
S20	55.196	9.500	57.870	10.31	49.520	8.520	46.350	7.940
S21	92.340	17.26	99.810	18.85	85.410	15.60	80.190	14.51
S22	88.000	16.57	94.260	17.93	80.880	14.92	75.910	13.90
S23	136.81	29.35	161.79	34.56	133.83	28.10	126.66	26.53

$$g_j(\alpha)=\int_0^{\alpha}\frac{d\alpha}{f_j(\alpha)}$$

where i is data point; β, v are the heating rate and its numbers; j is the numbers of the conversion function between 1 and 23. A plot $\ln\left[\frac{g_j(\alpha_{iv})}{T_{iv}^2}\right]$ *vs*. $\frac{1}{T_{iv}}$ for a given analytical form of $g(\alpha)$ should be a straight line. We use the twenty three different conversion functions given in Table 3 for the differential $f(\alpha)$ and integral $g(\alpha)$ functions in Eq. (4). 23 couples (Ea_{jv}, A_{jv}) of **L** and its metal complexes per heating rate, β are obtained by using the CR method and are listed in Tables 4–7.

The application of the IKP method is based on the study of the compensation effect. If a compensation effect is observed, a linear relation defined by Eq. (5) for each heating rate, is obtained. It is shown by plotting ln$A$ *vs*. E_a that a compensation effect is observed for each heating rate (Figs 8 and 9). Thus, using the relation of the compensation effect, for each heating rate the compensation parameters (α*, β*) are determined.

$$\ln A=\alpha^*+\beta^* E_a \qquad (5)$$

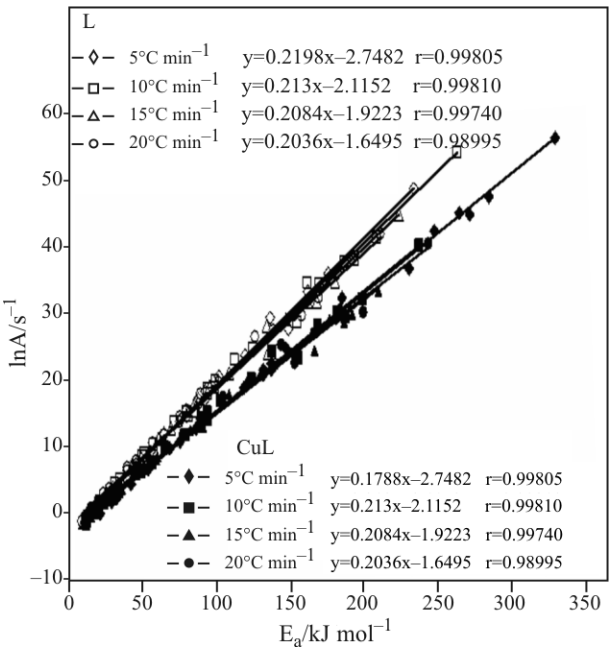

Fig. 8 Compensation effect for the L and CuL *vs*. heating rates

Table 5 Apparent conversion parameters of CuL obtained for various conversation functions by means of IKP method

Heating rate	5°C min^{-1}		10°C min^{-1}		15°C min^{-1}		20°C min^{-1}	
Function	E_a/kJ mol^{-1}	ln$A$/s^{-1}	E_a/kJ mol^{-1}	ln$A$/s^{-1}	E_a/kJ mol^{-1}	ln$A$/s^{-1}	E_a/kJ mol^{-1}	ln$A$/s^{-1}
S1	28.990	1.930	18.010	0.150	15.800	–0.17	18.050	0.690
S2	42.160	4.660	27.490	2.270	24.590	1.760	27.670	2.770
S3	68.510	9.860	46.450	6.160	42.170	5.290	46.910	6.620
S4	94.860	14.89	65.410	9.880	59.760	8.630	66.150	10.28
S5	147.55	24.76	103.34	17.09	94.930	15.07	104.64	17.37
S6	118.57	18.89	79.130	11.99	82.800	12.54	77.910	11.92
S7	132.00	21.62	90.020	14.30	88.650	13.76	89.740	14.35
S8	136.94	22.62	94.170	15.17	90.690	14.19	94.340	15.29
S9	247.66	42.25	168.69	28.16	176.20	29.10	166.64	26.90
S10	264.36	44.89	181.92	30.20	183.90	29.90	180.87	29.15
S11	270.99	44.70	187.44	29.43	186.46	28.73	186.94	29.20
S12	284.42	47.36	198.77	32.14	191.97	29.85	199.51	30.10
S13	230.32	36.55	155.96	23.29	166.35	24.61	153.54	22.56
S14	328.81	56.15	237.78	40.08	209.31	33.36	243.70	40.43
S15	21.740	0.230	11.965	–1.45	12.760	–0.98	11.370	–1.05
S16	32.500	2.510	19.420	0.310	20.550	0.780	18.760	0.670
S17	54.020	6.790	34.350	3.450	36.110	3.940	33.550	3.710
S18	75.530	10.90	49.280	6.380	51.670	6.880	48.340	6.530
S19	183.11	30.64	123.91	20.15	129.49	20.75	122.28	19.75
S20	86.290	12.92	56.740	7.800	59.460	8.320	55.730	7.900
S21	136.94	21.52	94.170	14.07	90.690	13.09	94.340	14.19
S22	132.00	20.93	90.020	13.60	88.650	13.07	89.740	13.66
S23	185.16	32.29	137.64	24.18	108.80	17.95	144.20	25.25

which leads to the supercorrelation relation

$$\alpha^* = \ln A_{int} - \beta^* Ea_{int} \quad (6)$$

where α^* and β^* are constants (the compensation effect parameters). A plot α^* *vs*. β^* is actually a straight line whose parameters allow evaluation of the invariant activation parameters (Fig. 10). Thus, the values of invariant activation energies and invariant pre-exponential factors can be calculated from the slopes and intercepts of curves.

The values of α^* and β^* obtained for **L** and each complexes are presented in Table 8.

The significance of α^* and β^* being characteristics of the experimental conditions has been demonstrated by Lesnikovich and Levchik [27].

Consequently, the values of the invariant activation energy and the invariant pre-exponential factor calculated from the slopes and intercepts of the straight lines obtained by using Eq. (6) presented in Table 9.

Complexes of Cu, Ni and Co show similar decomposition steps, the smaller size of Cu(II) as compared to Co(II) and Ni(II) permits a closer approach of the ligand to Cu(II) ion. Hence the E_{int} value for the Cu(II) complex is higher than that of Co(II) and Ni(II). The E_{int} values for thermal decomposition with respect

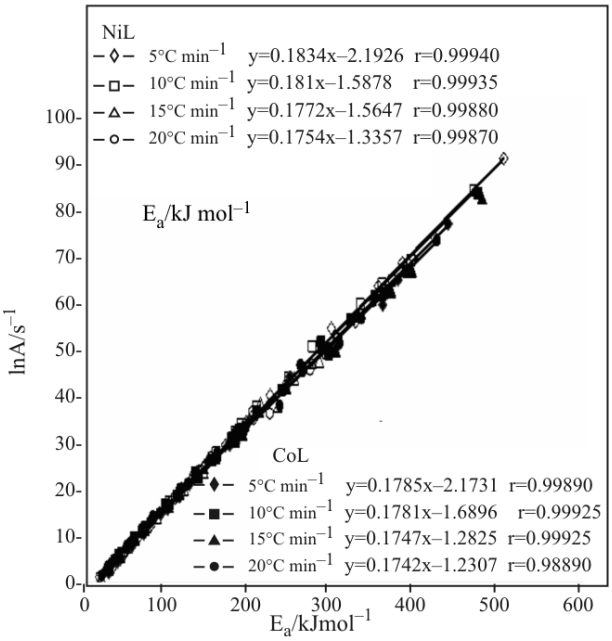

Fig. 9 Compensation effect for the NiL and CoL *vs*. heating rates

Table 6 Apparent conversion parameters of NiL obtained for various conversation functions by means of IKP method

Heating rate	5°C min^{-1}		10°C min^{-1}		15°C min^{-1}		20°C min^{-1}	
Function	E_a/kJ mol^{-1}	ln$A$/s^{-1}	E_a/kJ mol^{-1}	ln$A$/s^{-1}	E_a/kJ mol^{-1}	ln$A$/s^{-1}	E_a/kJ mol^{-1}	ln$A$/s^{-1}
S1	357.41	63.84	336.23	59.78	255.52	44.19	246.93	42.48
S2	386.97	68.95	363.15	64.33	276.85	47.65	267.60	45.78
S3	399.20	69.84	374.25	64.98	285.72	47.86	276.12	45.92
S4	424.18	74.72	396.90	69.38	303.88	51.38	293.50	49.26
S5	329.46	56.10	310.42	52.49	235.49	38.03	227.33	36.43
S6	509.23	91.29	473.82	84.26	365.95	63.35	352.42	60.54
S7	226.86	40.47	211.28	37.70	161.15	28.06	155.18	26.95
S8	147.69	25.51	137.28	23.87	103.83	17.47	99.800	16.81
S9	108.12	17.94	100.29	16.86	75.150	12.07	72.100	11.63
S10	68.530	10.22	63.290	9.704	46.490	6.520	44.400	6.290
S11	48.740	6.250	44.790	6.000	32.160	3.610	30.560	3.490
S12	173.39	29.87	162.77	28.15	122.35	20.40	117.97	19.65
S13	197.62	34.69	184.79	32.50	139.87	23.87	134.88	22.98
S14	206.78	36.50	193.10	34.14	146.53	25.18	141.26	24.23
S15	81.380	12.50	76.030	11.94	55.750	8.080	53.490	7.820
S16	50.710	6.480	47.120	6.311	33.560	3.730	32.000	3.620
S17	35.380	3.350	32.660	3.370	22.460	1.410	21.250	1.370
S18	112.05	18.36	104.94	17.41	77.950	12.26	74.980	11.84
S19	265.40	46.92	249.50	44.03	188.94	32.36	182.45	31.13
S20	127.39	21.25	119.40	20.11	89.050	14.31	85.730	13.81
S21	300.95	55.01	278.13	50.74	215.46	38.64	206.34	36.86
S22	197.62	33.99	184.79	31.81	139.87	23.18	134.88	22.29
S23	206.78	35.40	193.10	33.04	146.53	24.08	141.26	23.14

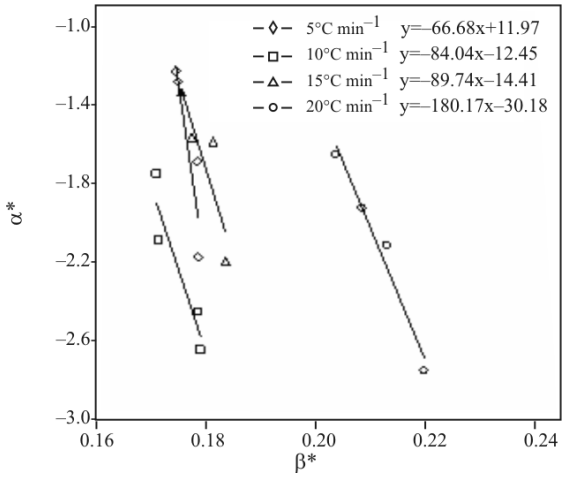

Fig. 10 Verifying supercorrelation relation (Eq. (6))

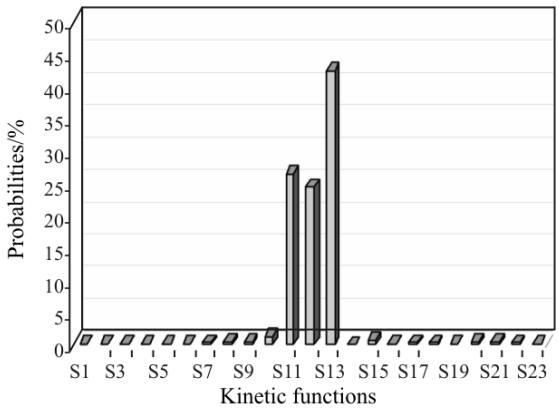

Fig. 11 Probability distribution of the kinetic decomposition functions of **L** computed with IKP method

to the above method can be put into a descending order as, E_{Cu}>E_{Ni}>E_{Co}>**L**. The activation energies' corresponding decomposition steps are in the range of 66.68–180.17 kJ mol^{-1}. On the other hand, the probabilities of the j^{th} function, P_j, which may characterize the mode of decomposition of each sample, was discussion. The P_j are computed with the assumption that the experimental data with conversion function are described by a complete and independent event system. The probabilities of j^{th} function, P_j, developed by Bourbigot [28, 29] for the decomposition process can be calculated by defining the ration $F_j^2 = \frac{S_j^2}{S_m^2}$ using A_{inv} and

Table 7 Apparent conversion parameters of CoL obtained for various conversation functions by means of IKP method

Heating rate	5°C min^{-1}		10°C min^{-1}		15°C min^{-1}		20°C min^{-1}	
Function	E_a/kJ mol^{-1}	ln$A$/s^{-1}	E_a/kJ mol^{-1}	ln$A$/s^{-1}	E_a/kJ mol^{-1}	ln$A$/s^{-1}	E_a/kJ mol^{-1}	ln$A$/s^{-1}
S1	41.900	4.660	44.460	5.770	44.970	6.090	37.700	4.910
S2	59.460	8.160	62.920	9.400	63.660	9.700	54.030	8.120
S3	94.570	14.94	99.840	16.44	101.06	16.70	86.100	14.29
S4	129.69	21.57	136.77	23.32	138.45	23.55	119.36	20.30
S5	199.92	34.62	210.61	36.90	213.24	37.04	184.70	32.13
S6	159.75	26.71	156.86	26.50	160.98	27.11	127.73	21.31
S7	178.46	30.41	180.80	31.15	184.50	31.59	153.47	26.22
S8	185.30	31.75	190.03	32.93	193.47	33.30	163.25	28.08
S9	330.26	57.63	324.64	56.55	333.08	57.37	266.76	45.47
S10	353.62	61.48	353.47	61.38	361.63	62.05	298.05	50.61
S11	362.81	59.76	365.74	62.22	373.59	62.79	311.11	51.53
S12	381.37	65.36	390.99	67.03	398.07	67.37	337.79	56.85
S13	305.76	50.62	298.41	49.27	306.49	50.11	239.03	38.02
S14	442.34	77.15	479.01	83.74	482.12	83.06	428.76	73.73
S15	31.860	2.460	31.020	2.880	31.900	3.330	23.460	1.830
S16	46.070	5.350	45.010	5.700	46.240	6.170	35.040	4.210
S17	74.490	10.86	72.970	11.07	74.930	11.57	58.210	8.670
S18	102.91	16.21	100.93	16.28	103.61	16.82	81.390	12.95
S19	245.00	42.24	240.75	41.59	247.03	42.30	197.25	33.38
S20	117.12	18.86	114.92	18.86	117.95	19.41	92.980	15.06
S21	185.30	30.66	190.03	31.84	193.47	32.20	163.65	26.80
S22	178.46	29.71	180.80	30.45	184.50	30.90	153.47	25.96
S23	251.19	44.63	288.89	51.88	287.06	50.93	264.19	46.72

Table 8 The values of α* and β* for **L**, CuL, NiL and CoL *vs.* heating rates

β/°C min^{-1}	**L**			CuL		
	α*	β*	*r*	α*	β*	*r*
5	–2.7482	0.2198	0.99805	–2.6420	0.1788	0.99750
10	–2.1152	0.2130	0.99810	–2.4496	0.1783	0.99700
15	–1.9223	0.2084	0.99740	–2.0882	0.1711	0.99720
20	–1.6495	0.2036	0.98995	–1.7482	0.1708	0.99190
β/°C min^{-1}	NiL			CoL		
	α*	β*	*r*	α*	β*	*r*
5	–2.1926	0.1834	0.99940	–2.1731	0.1785	0.99890
10	–1.5878	0.1810	0.99935	–1.6896	0.1781	0.99925
15	–1.5647	0.1772	0.99880	–1.2825	0.1747	0.99925
20	–1.3357	0.1754	0.99870	–1.2307	0.1742	0.99890

r–regression coefficient

Ea_{inv} values obtained, where $S_j^2 = \frac{1}{p}\sum_{i=1}^{v=p} S_{jv}^2$ and S_m is the average minimum of residual dispersion. This ratio obeys the F-distribution. Having n of the i^{th} of the experimental values of $(d\alpha/dT)_{iv}$, the residual sum of squares for each $f_i(\alpha)$ and for each heating rate β_v may be computed as

$$(n-1)S_{jv}^2 = \sum_{i=1}^{i=n}\left|\left(\frac{d\alpha}{dT}\right)_{iv} - \frac{A_{inv}}{\beta_v}\exp\left(\frac{E_{inv}}{RT_{iv}}\right) f_i(\alpha_{jv})\right|^2 \quad (6)$$

Table 9 Invariant kinetic parameters obtained for the salen type salicylaldimine ligand and complexes at different heating rate by means of CR method

Sample	E_{inv}/kJ mol^{-1}	A_{inv}/s^{-1}
L	66.68	$1.5 \cdot 10^5$
CoL	84.04	$2.5 \cdot 10^5$
NiL	89.74	$1.8 \cdot 10^6$
CuL	180.17	$1.2 \cdot 10^{13}$

where n is the number of degrees of freedom equal for every dispersion.

The kinetic pairs (A_{inv} and Ea_{inv}) and probabilities for twe decomposition functions were carried out with software developed in our laboratory using Excel 2000. The histogram showing the distribution of the probabilities associated with the twenty-three decomposition functions is presented for **L** in Fig. 11.

The kinetic functions of the four materials are close. From the distribution of probabilities can be shown that the diffusion functions (D_n) are most probable for the thermal decomposition of each sample. The histograms obtained from differential methods are also similar that of integral method.

Conclusions

The TG curves of all the compounds show similar decomposition when heated to about 500°C. The complexes prepared with different metals decompose via a one-step process. It was found that the thermal stabilities of the ligand and its metal complexes follow the order Co(II)>Cu(II)>Ni(II)>**L**. Using the IKP method a kinetic analysis of the thermogravimetric data was performed. The activation energy of the complexes determined by applying Coats and Redfern method and increased in the order Co(II)<Ni(II)<Cu(II). Also, the activation energy of **L** and the complex samples studied was in the range of 66–180 kJ mol^{-1} depending on the heating rate and model assumptions. The kinetic function related to the mode of decomposition of all complexes was found to be close. The diffusion functions (D_n) are most probable for the thermal decomposition of all complexes. DIP-MS was found to be very powerful technique for the characterization of the complex structure. It was noticed that doubly charged ion stability occurred via two methyl groups leaving from both sides of the ligand and its metal ion complexes was high.

Acknowledgements

The authors gratefully acknowledge Basri Gülbakan and Ömür Çelikbiçak for helpful Mass Spectrometry measurements.

References

1 W. Zhang, J. L. Loebach, S. R. Wilson and E. N. Jacobsen, J. Am. Chem. Soc., 112 (1990) 2801.
2 T. Matsuura, Tetrahedron, 33 (1977) 2869.
3 J. L. Serrano and L. Oriol, Adv. Mater., 7 (1995) 365.
4 L. Mao, K. Yamamato, W. Zhou and L. Jin, Electroanalysis, 12 (2000) 72.
5 J. F. Larrow, E. N. Jacobsen, Y. Gao, Y. Hong, X. Nie and C. M. Zepp, J. Org. Chem., 59 (1994) 1939.
6 J. Madarász, G. Pokol and S. Gál, J. Thermal Anal., 42 (1994) 539.
7 I. L. Lapides, J. Thermal Anal., 50 (1997) 269.
8 F. Carrasco, Thermochim. Acta, 213 (1993) 115.
9 M. V. Kök and N. Acar, J. Therm. Anal. Cal., 83 (2006) 445.
10 M. V. Kök, J. Therm. Anal. Cal., 88 (2007) 663.
11 M. V. Kök and A. G. Iscan, J. Therm. Anal. Cal., 88 (2007) 657.
12 J. Zsakó, J. Thermal Anal., 46 (1996) 1854.
13 A. A. Soliman, S. M. El-Medani and O. A. M. Ali, J. Therm. Anal. Cal., 83 (2006) 385.
14 S. Durmuş, Ü. Ergün, J. C. Jaud, K. C Emregül, H. Fues and O Atakol, J. Therm. Anal. Cal., 86 (2006) 337.
15 O. Z. Yeşilel, H. Ölmez and H. İçbudak, J. Therm. Anal. Cal., OnlineFirst DOI: 10. 1007/s10973-005-7479-9.
16 G. G. Mohamed and H. Z. El-Wahab, J. Therm. Anal. Cal., 73 (2003) 347.
17 F. Doğan, S. Gülcemal, M. Yürekli and B. Çetinkaya, J. Therm. Anal. Cal., 91 (2008) 395.
18 V. T. Kasumov and F. Koksal, Spectrochim. Acta, Part A, 61A(1-2) (2004) 225.
19 V. T. Kasumov, S. O.-Yaman and E. Tas, Spectrochim. Acta, Part A, 62A(1-3) (2005) 716.
20 S. V Levchik, G. F. Levchik and A. L. Lesnikovich, Thermochim. Acta, 92 (1985) 157.
21 M. Arshad, Saeed-ur-Rehman, S. Ali Khan, K. Masud, N. Arshad and A. Ghani, Thermochim. Acta, 364 (2002) 143.
22 G. G. Mohamed, F. A. Nour-El Dien and E. A. El-Gamel, J. Therm. Anal. Cal., 67 (2002) 135.
23 F. Doğan, M. Ulusoy, Ö. F. Öztürk, I. Kaya and B. Salih, J. Therm. Anal. Cal., (2009), in print.
24 V. Mamleev, S. Bourbigot, M. Le Bras, S. Duquesne and J. Sešták, Phys. Chem. Chem. Phys., 2 (2000) 4708.
25 A. J. Lesnickovick and S. V Levchick, J. Thermal Anal., 30 (1985) 667.
26 A. W. Coats and J. P. Redfern, Nature, 201 (1964) 68.
27 A. J. Lesnickovick and S. V Levchick, J. Thermal Anal., 27 (1983) 83.
28 S. Bourbigot, R. Delobel, M. Le Bras and D. Normand, J. Chim. Phys., 90 (1993) 1909.
29 S. Bourbigot, X. Flambard and S. Duquesne, Polym. Int., 50 (2001) 157.

Received: January 7, 2008
Accepted: September 16, 2008

DOI: 10.1007/s10973-008-8980-8